DALTON

Mössbauer and electron paramagnetic resonance studies on some new bis-(ligated) porphyrinatoiron(III) complexes with aliphatic amines. Models for cytochromes b

Paul J. Marsh, Jack Silver,* Martyn C. R. Symons* and Fatai A. Taiwo

Department of Biological and Chemical Sciences, Central Campus, University of Essex, Wivenhoe Park, Colchester CO4 3SQ, UK

A series of bis(axially ligated) complexes $[Fe^{III}L^1(L')_2]^+$ (H_2L^1 = 3,7,12,17-tetramethyl-8,13-divinylporphyrin-2,18-dipropanoic acid; L' = ethyl-, *n*-propyl-, *n*-butyl-, *n*-octyl-, *n*-decyl-, *n*-dodecyl-, *n*-octadecyl-amine, 1,2-diaminoethane, morpholine or piperidine) have been prepared in solution and their electronic absorption, EPR and Mössbauer spectra recorded in solution or frozen solution. The electronic spectra indicate that new porphyrinato complexes have been prepared. The Mössbauer spectroscopic data show these to be low-spin iron(III) complexes, with smaller quadrupole splittings than those previously reported for similar N-heterocyclic complexes. The Mössbauer data when compared to those of the iron(II) analogues as well as to those of pyridine, imidazole and histidine complexes [both iron-(II) and -(III)] facilitate a more comprehensive understanding of the bonding of all the compounds. [This work allowed insight into the σ-bonding component of the axial ligands in bis(ligated) imidazole and histidine complexes of (protoporphyrinato IX)iron(III).] The π-donor ability of imidazole and histidine ligands and its effect on iron(III) porphyrins is manifest. The EPR spectra for the aliphatic amine complexes at 77 K are characteristic of low-spin iron(III). In several cases two similar sets of *x*, *y* and *z* features were obtained, indicative of two alternative conformers. The intermediate *g* values were all close to 2.20. The maximum values were in the range 2.51–2.77 and the minimum values in the range 1.79–1.90. These *g* shifts are the smallest on record for complexes of this type, which requires some mechanism for strongly lifting the $d_{xz,yz}$ orbital degeneracy. Conventionally, this splitting is discussed in terms of π bonding involving the fifth and sixth ligands, but the amine ligands here are not able to participate in π bonding. A lateral movement of these ligands is tentatively invoked such that one (say d_{yz}) of the d orbitals is involved in σ bonding.

In previous studies we have described models for cytochrome b proteins based on complexes of (protoporphyrinato IX)-iron(III), $[FeL^1]^+$ (H_2L^1 = 3,7,12,17-tetramethyl-8,13-divinyl-porphyrin-2,18-dipropanoic acid), with imidazoles, substituted imidazoles,[1] and also histidine[2] and its substituted derivatives.

Extensive studies on the nature of the axial ligands of cytochromes b from various mitochondrial and chloroplast sources have demonstrated that the haem in these proteins is co-ordinated to two histidine residues.[3-10] In fact cytochrome b_5 from liver[4] and erythrocytes of animals[5] chloroplast[6,7] cytochrome b_6 and b_{559}, yeast flavocytochrome b_2,[8] mitochondrial b_{562} (b_K) and b_{566} (b_T) and cytochrome a of cytochrome oxidase[9,10] have all been identified as having these axial ligands. The steric and electronic influences of these ubiquitous histidine ligands are the primary mechanisms of fine control of haem iron reactivity in haemoproteins.[11]

A wide variety of physical properties[12-15] found in the cytochrome proteins, has been ascribed to differences in orientation of the two imidazole planes of histidine,[7,14,16-18] steric strain of bis(histidine) ligation,[13,14] or hydrogen bonding of axial histidines.[15,16] A secondary but no less powerful control mechanism that has also been postulated to exist involves perturbation of the porphyrin ring by various π donor–acceptor[19] interactions between the haem and an aromatic residue such as histidine, phenylaniline or tyrosine.

In our Mössbauer spectroscopic study of $[FeL^1(L')_2]^+$ (L' = imidazole or substituted imidazole) complexes in various solvents we found a relationship between the orientation of the axial imidazole plane and the observed quadrupole splitting (ΔE_Q) and line shapes.[1] Large ΔE_Q values of around 2.34–2.43 mm s^{-1} were assigned to structures where the two imidazoles are more or less parallel in alignment, whereas values around 1.8 mm s^{-1} were assigned to perpendicular orientation of the imidazole planes. In a similar study on bis(histidine) and related complexes we demonstrated that the histidine ligands bind as sterically hindered imidazoles and that the iron–imidazole bonds are weak.[2] The magnitude of the ΔE_Q value of 2.14 mm s^{-1} and large linewidths suggested that the two imidazole planes are non-parallel but with a large angle between the planes.[2] Other workers have since reached similar conclusions in regard to the assignment of the Mössbauer and also EPR parameters.[20,21] The observation of asymmetric quadrupole doublets together with broad lines is characteristic of slow spin–lattice relaxation of iron similar to that observed for cytochrome c[22] and small peptides prepared there from.[23-25] In such cases $T_1 \leqslant 10^{-8}$ s at 77 K. The resulting Mössbauer spectroscopic data for the bis(histidine) complexes were similar to those found for low-spin iron(III) cytochromes[22,26] and cytochrome b_5.[27] Furthermore these studies demonstrated that steric strain arising from the histidine side chains and electrostatic interactions between the charged groups and the porphyrin propionate carboxylates influenced the iron electronic structure and the imidazole plane orientations.[2]

The results of these studies[1,2] together with those of related work[1,6,7,12-18,20,21,28] may eventually lead to an understanding of the various possible roles of the side chains attached to the imidazole ring of the histidine residues in controlling the electronic structure of iron in the cytochromes b. However, one aspect of the overall nitrogen ligation of $[FeL^1(L')_2]$ complexes (L' = imidazole or histidine ligands) that has not been explored is what is the contribution of the π cloud on the ligands to the bonding of the iron atom, and concomitant with this, what is the σ-bonding contribution? In this paper we report the first studies of a range of bis(aliphatic amine) complexes of $Fe^{III}L^1$ that attempt to cast light on these questions.

Previous literature[29] has shown that aliphatic amines bind $Fe^{II}L^1$ much less strongly than N-heterocycles.[30] Moreover the binding constants of N-heterocycles to iron(III) porphyrins have been shown to be very much smaller than those of the corresponding iron(II) complexes,[31a] so that the possible formation of bis(aliphatic amine) complexes of iron(III) porphyrins has been ignored if not dismissed, until very recently. The first directly measured equilibrium constants for bonding of $Fe^{III}L^1$ in the absence of protein with aliphatic amines in both axial sites used ethanolamine.[31b] A number of elegant papers that show aliphatic amines bonding the iron(III) porphyrin of microperoxidase have also recently been published, though in these the other axial ligand is a histidine residue.[31c-e] In addition similar work has been carried out on the binding studies of vitamin B_{12}.[31f] We report in this work Mössbauer, electron paramagnetic resonance and electronic absorption spectroscopic studies of complexes $[Fe^{III}L^1(L')_2]^+$ (L' = ethyl-, *n*-propyl-, *n*-butyl-, *n*-octyl-, *n*-decyl-, *n*-dodecyl-, *n*-octadecyl-amine, 1,2-diaminoethane, morpholine or piperidine) in solutions at pH 10, and discuss the results in comparison with the known $[Fe^{II}L^1(L')_2]$ complexes (L' = aliphatic amines and N-heterocycles) and $[Fe^{III}L^1(L')_2]^+$ complexes where L' = N-heterocycles.

Experimental

Preparation of haematin–aliphatic amine complexes

Haematin, $[Fe^{III}L^1(OH)]$, and all amines used were obtained from Aldrich Chemicals or Pharmacos (1,2-diaminoethane), absolute alcohol A.R. from Hayman, and methanol from Fisons. All chemicals were used without further purification.

Haematin (0.20 g) was dissolved, at room temperature, in a solution of the appropriate amine: (*i*) low-boiling liquid amines (*i.e.* ammonia, methyl-, dimethyl-, ethyl-, diethyl-, triethyl-, *n*-propyl- or *n*-butyl-amine) as the neat solutions where possible or as the amine dissolved in water ($\approx$200 cm^3); (*ii*) high-boiling liquid amines (*i.e.* *n*-octyl-, *n*-decyl-amine, piperidine or 1,2-diaminoethane) or solid amines (*i.e.* *n*-dodecyl- or *n*-octadecyl-amine) as solutions ($\approx$20 mole equivalents of haematin used) in absolute alcohol ($\approx$200 cm^3). Better product yields were obtained when the haematin–amine solution (intense red) was allowed to stand, at room temperature, overnight. Air was bubbled through the solutions for several hours (slight change from intense red to darker red-brown). The solutions were then reduced in volume by rotary evaporation to $\approx$5–10 cm^3. Such concentrated solutions were suitable for Mössbauer spectroscopy.

Mössbauer measurements

Mössbauer spectra were recorded using frozen solutions at 77 K. The apparatus and fitting methodology have been described previously.[32]

EPR measurements

Methanol was added to the concentrated haematin–amine solutions, which were then immediaely frozen as droplets in liquid nitrogen to produce glassy pellets for EPR measurements. The same results were obtained even in the absence of methanol. The pellets were loaded into a finger Dewar filled with liquid nitrogen.

First-derivative EPR spectra were obtained, at 77 K, on a Varian E109 X-band spectrometer set at 100 kHz modulation frequency. The scan range and field sweep were set to cover the high- and low-field regions (g = 6 to 2). Two scans were routinely used, one covering the whole field range to monitor features, if any, in the g = 6 and 4 regions, and the other covering the main features in the g = 2 to 1 range. The spectra were accumulated on an Archimedes 440 computer interfaced with the spectrometer. Spectra were calibrated with acetylacetonatoiron(III) and diphenylpicrylhydrazyl (dpph) crystals for the g = 4.3 and free-spin regions respectively. For broad overlapping features g values were estimated by simulation.

Results and Discussion

To enable bis(aliphatic amine) complexes of the type $[Fe^{III}L^1(L')_2]^+$ to be prepared the strategy was to carry out the studies in basic solution, *i.e.* in the range pH 10–11 (for aqueous media) and always above the pK_a of the aliphatic amine to ensure that free amine was present. At these pH values in iron(III) solution the major species is the μ-oxo dimer of $Fe^{III}L^1$.[32a] Thus free unprotonated amine competes as an axial ligand for iron(III) even in the presence of the μ-oxo dimer. The latter is autoreduced by the excess of amine to iron(II),[33a] which complexes the amine and is reoxidised to $[Fe^{III}L^1(L')_2]^+$ on passing air through the solution. This was demonstrated by frozen-solution Mössbauer spectroscopy (at 77 K) and electronic absorption spectroscopy (at room temperature) (see Tables 1 and 2). From Table 1 the electronic absorption spectra for all the complexes can be seen to be very similar and are quite different from those of the corresponding low-spin iron(II) species[29] and also from that of the μ-oxo dimer of $Fe^{III}L^1$.[32a] There is evidence (Table 1) that ethylamine forms a bis complex with $Fe^{III}L^1$ in the dilute solution used for the electronic absorption spectroscopic data, however, the spectrum lacks the shoulder seen at 470 nm from the other complexes. No evidence for this complex could be found in the more concentrated solutions used for Mössbauer spectroscopy; EPR only showed a broad diffuse spectrum (see below). These facts may be taken as evidence that the species only forms to a minor extent.

It was found to be impossible to produce $[Fe^{III}L^1(L')_2]^+$ complexes for L' = ammonia, methyl-, ethyl-, dimethyl-, diethyl- or triethyl-amine by either method, and as already mentioned we only found evidence for a complex for L' = ethylamine in the electronic absorption spectrum. We are not completely certain why the small amines did not give complexes but suggest that it may be because ammonia and ethylamine have heats of hydration which are much larger than those of the longer-chain amines.[34] Thus their interactions with water, *i.e.* degree of hydration, are greater and it is this that limits their ability to form $[Fe^{III}L^1(L')_2]^+$ complexes. We also suggest that the failure to form such complexes with dimethyl- or triethyl-amine may be due to steric effects.

Table 1 Electronic absorption spectroscopic data for complexes in ethanol and relevant literature data

L' Complex	Soret band (nm)	Other bands (nm)		
$[Fe^{III}L^1(L')_2]$				
Ethylamine	396	—	591	—
n-Propylamine	399	468[a]	590	670
n-Butylamine	401	470[a]	590	675
n-Octylamine	400	480[a]	592	—
n-Decylamine	398	470[a]	593	—
n-Dodecylamine	398	470[a]	592	—
n-Octadecylamine	399	471[a]	597	—
1,2-Diaminoethane	398	—	591	—
Morpholine	398	470[a]	590	—
Piperidine	398	465[a]	591	—
$[(Fe^{III}L^1)_2O]$[b]	387		608	
$[Fe^{II}L^1(L')_2]$[c]				
n-Propylamine	421	525	556	
n-Butylamine	420	526	556	
n-Octylamine	420	526	556	

[a] Weak shoulder. [b] Ref. 32(*a*). [c] Ref. 29.

Table 2 Frozen-solution Mössbauer spectroscopic data at 77 K for $[Fe^{III}L^1(L')_2]^+$ complexes prepared in this work

L'	δ^a/mm s^{-1}	ΔE_Q/mm s^{-1}	Γ^b/mm s^{-1}	% Effect[c]
Ethylamine[d]	0.38(1)	0.56(1)	0.21(2)	100
n-Propylamine	0.24(2)	1.49(5)	0.38(4)	80(10)
d	0.40(1)	0.58(1)	0.15(3)	20(5)
n-Butylamine	0.25(3)	1.80(3)	0.24(3)	59(4)
e	0.44(3)	1.05(3)	0.15(3)	33(2)
d	0.40(2)	0.58(2)	0.14(4)	8(1)
n-Octylamine	0.25(1)	1.63(2)	0.25(2)	70(5)
d	0.40(1)	0.58(1)	0.19(2)	30(3)
n-Decylamine	0.28(2)	1.64(2)	0.20(1)/0.30(3)[f]	90(7)
d	0.40(1)	0.58(2)	0.18(5)	10(4)
n-Dodecylamine	0.23(1)	1.61(1)	0.24(1)	71(4)
d	0.36(1)	0.58(2)	0.17(1)	29(3)
1,2-Diaminoethane	0.28(2)	1.64(2)	0.20(2)/0.40(4)[f]	100
Morpholine	0.32(2)	2.01(2)	0.18(1)/0.37(3)[f]	71(5)
d	0.40(1)	0.58(1)	0.17(1)	29(3)
Piperidine	0.41(7)	2.13(8)	0.36(5)/0.51(13)[f]	35(7)
d	0.41(1)	0.58(1)	0.27(2)	63(5)

[a] Relative to metallic iron at 298 K. [b] Half width at half height. [c] The amount of each site's contribution to the total iron observed in the spectrum, taken from the computer fit. [d] μ-Oxo dimer of $Fe^{III}L^1$. [e] Low-spin $Fe^{II}L^1$. [f] A two-line fit was necessary as spin–lattice relaxation leads to broadening of the high-energy lines.

Table 3 Frozen-solution Mössbauer spectroscopic data for $[Fe^{III}L^1(L')_2]^+$ complexes at 77 K

L'	Solvent	δ^a/mm s^{-1}	ΔE_Q/mm s^{-1}	Γ^b/mm s^{-1}	Ref.
Imidazole	Me_2SO	0.22(2)	2.38(2)	0.21(3)/0.26(4)	2
	Water–ethanol (1 : 1)	0.24(1)	2.35(1)	0.31(1)/0.32(1)	2
	Solid	0.24	2.30	Not given	33
1-Methylimidazole	Water–ethanol (1 : 1)	0.26(1)	2.34(1)	0.16(1)/0.18(1)	2
	Me_2SO	0.23(1)	2.24(1)	0.37(1)/0.49(2)	2
2-Methylimidazole	Water–ethanol (1 : 1)	0.16(2)	1.87(2)	0.29(1)/0.59(3)	2
Histidine	Water (pH 10.1)	0.26(6)	1.99(6)	0.19(8)/0.30(9)	1
N^{α}-Acetylhistidine	Ethanol–water (pH 8.4)	0.21(3)	2.09(3)	0.40(3)/0.61(6)	1
Histamine (imidazole-4-ethanamine)	Water (pH 11.0)	0.28(5)	2.28(5)	0.32(4)/0.42(8)	1
Pilocarpate[c]	Water (pH 10.1)	0.26(2)	2.22(2)	0.36(2)/0.44(4)	1
Pyridine	Solid	0.23	1.88	Not given	33

[a] Relative to metallic iron at 298 K. [b] Half width at half height. [c] 2-Ethyl-3-hydroxymethyl-4-(1-methylimidazol-5-yl)butanoate.

Mössbauer data

The Mössbauer spectroscopic results for the frozen solutions studied are presented in Table 2. For comparative purposes those of some $[Fe^{III}L^1(L')_2]^+$ complexes (L' is a N-heterocycle) [1,2,33b] are presented in Table 3. The following observations can be made by comparing the data in the two tables: (1) the ΔE_Q values of the non-cyclic aliphatic amine complexes in Table 2 are smaller than those of the N-heterocycle complexes in Table 3; (2) the chemical shifts of the aliphatic amines in Table 2 are similar to those of the N-heterocycles in Table 3; and (3) the ΔE_Q data for the piperidine and morpholine complexes are much larger than those of the other aliphatic amines.

Table 4 presents Mössbauer spectroscopic data for a number of N-heterocyclic and aliphatic amine complexes of general formulae $[Fe^{II}L^1(L')_2]$ [which are the same or similar to compounds of the iron(III) analogues in Tables 2 and 3]. The geometry of the iron(II) complexes can be considered as that shown in Scheme 1 where the axial ligands are amines or N-heterocycles. From Table 4 it can be seen that: (*a*) all the aliphatic amine compounds [29,30,35] other than piperidine have smaller ΔE_Q values than the pyridine-type N-heterocycles [just as is observed for the iron(III) complexes], however, the aliphatic amine ligands have larger ΔE_Q values than the non-sterically hindered five-membered ring imidazole ligands; (*b*) the chemical shifts tend to be larger for the aliphatic amines compared with the N-heterocycles [not in accord with the iron(III) complexes]; and (*c*) the ΔE_Q data for the piperidine complex are larger than those of the non-cyclic aliphatic amines [as observed for the iron(II) complexes in this work].

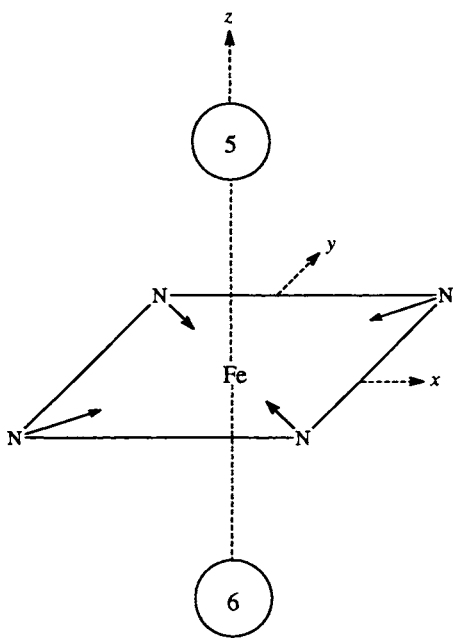

Scheme 1 The circles represent the fifth and sixth (axial) co-ordination sites

The range of ΔE_Q values for the iron(II) complexes with aliphatic amines (apart from piperidine) is 1.03(1) to 1.09(1) mm s^{-1} with a spread of around 0.06(2) mm s^{-1}, whereas for the

Table 4 Mössbauer spectroscopic data for $[Fe^{II}L^1(L')_2]$ complexes in frozen solution at 77 K

L'	δ^a/mm s^{-1}	ΔE_Q/mm s^{-1}	Γ^b/mm s^{-1}	Ref.
Methylamine	0.47(1)	1.08(1)	0.17(1)	29
Ethylamine	0.47(3)	1.09(1)	0.17(1)	29
n-Propylamine	0.49(1)	1.09(1)	0.22(1)	29
n-Butylamine	0.48(1)	1.03(1)	0.17(1)	29
n-Octylamine	0.48(2)	1.09(1)	0.13(1)	29
Piperidine	0.49(1)	1.43(1)	0.14(1)	This work
Imidazole	0.43(1)	0.96(1)	0.19(1)	30
1-Methylimidazole	0.47(1)	1.03(1)	0.15(1)	35(*a*)
2-Methylimidazole	0.51(2)	1.26(3)	0.21(3)	35(*a*)
5-Chloro-1-methylimidazole	0.43(1)	0.97(2)	0.17(1)	30
Histidine	0.42(2)	1.02(3)	0.16(2)	35(*b*)
N^{α}-Acetylhistidine	0.44(2)	1.04(2)	0.18(2)	35(*b*)
Pilocarpate	0.46(1)	1.04(2)	0.16(2)	35(*b*)
Histamine	0.48(2)	1.04(3)	0.25(2)	35(*b*)
Pyridine	0.45(1)	1.21(1)	0.18(1)	30
4-Methylpyridine	0.48(1)	1.17(1)	0.17(1)	30
3,4-Dimethylpyridine	0.46(1)	1.15(1)	0.15(1)	30
4-Chloropyridine	0.46(1)	1.23(1)	0.24(1)	30
3-(Aminomethyl)pyridine	0.45(1)	1.14(1)	0.17(1)	30
Isoquinoline	0.43(1)	1.11(1)	0.13(1)	30

[a] Relative to metallic iron at 298 K. [b] Half width at half height.

iron(III) complexes the range is 1.49(5)–1.80(3) mm s^{-1} with a total spread of around 0.30(5) mm s^{-1}. For the iron(II) pyridine complexes the spread in ΔE_Q is 0.12(2) mm s^{-1}, whereas for iron(III) it is again larger, around 0.20 mm s^{-1} [derived from the data in Table 3, and those for the pyridine attached to $Fe^{III}L^1$ (ref. 21) and 4,*N*-dimethylpyridine attached to Fe^{III}(tmp) (tmp = 5,10,15,20-tetramethylporphyrinate) (ref. 20)]. We have neglected those for the oep[20] (2,3,7,8,12,13,17,18-octaethylporphyrinate) which has a parallel ligand arrangement and tpp[33] (5,10,15,20-tetraphenylporphyrinate) complexes in which the pyridine ligands are nearly perpendicular to each other, but the ground state is not $(3d_{xy})^2(3d_{xz}, 3d_{yz})^3$ (see later). The larger magnitude of ΔE_Q for the iron(III) compounds arises from the fact that the low-spin iron(III) complexes have one less electron in the t_{2g} orbitals than do the iron(II) compounds. (We have previously discussed this in detail.[1,2]) The quadrupole splitting is made up of two terms, $\Delta E_Q = q_{valence} + q_{lattice}$ where $q_{valence}$ is the electric field due to the valence electron and $q_{lattice}$ is the field generated by all other charges in the lattice. The net result for the iron(III) compounds is that there is a large valence contribution to ΔE_Q, but relatively little direct valence effect in the iron(II) complexes. In the latter the major contribution to V_{zz} (the principal component of the electronic field gradient) comes from the imbalance in the iron $3d_{x^2-y^2}$ and $3d_{z^2}$ orbitals due to σ-bonding interactions,[36] and the positive signs found for V_{zz} indicate that the covalent bonding to the planar porphyrin is stronger than that to the axial ligands.[37,40]

The relationship between ΔE_Q and V_{zz} is as in equation (1),

$$\Delta E_Q = \left(\frac{eQ}{2} V_{zz}\right)\left(1 + \frac{\eta^2}{3}\right)^{\frac{1}{2}} \quad (1)$$

where e is the charge of the proton, Q is the nuclear quadrupole moment and η is the asymmetry parameter. In every case η is nearly or exactly zero.[37,40]

In this discussion on the origins of ΔE_Q we deal only with contributions made by metal 3d orbitals, and choose to ignore the metal 4p orbitals. There is no strong evidence for significant involvement of the latter in the bonding of six-co-ordinate iron porphyrin complexes,[41] and in our view, they can be safely ignored.

Interestingly V_{zz} has also been found to be positive in some low-spin $[Fe^{III}(por)(L')_2]^+$ complexes (por = tpp or oep type porphyrins and L' = a N-heterocycle).[16,20,42] In these cases where the ground state has been ascribed to $(3d_{xy})^2(3d_{xz}, 3d_{yz})^3$ the covalent bonding to the planar porphyrin is also stronger than that to the axial ligands. Thus, there is no difference in the sign of the field gradient for iron-(II) and -(III).

The parameter V_{zz} is given approximately by equation (2),[41a,43] where the n values are the effective populations of the

$$V_{zz} = K[n_{x^2-y^2} - n_{z^2} + n_{xy} - \tfrac{1}{2}(n_{xz} + n_{yz})] \quad (2)$$

appropriate 3d orbitals. Since the d_{xy} orbitals are almost non-bonding, n_{xy} can be treated as a constant.

For the aliphatic amines, as the σ-donor strength of the axial ligands increases the asymmetry of the field generated by σ bonding will decrease and a smaller ΔE_Q will be observed. If an axial ligand has a low-lying π* orbital then this will be able to interact with the filled d_{xz} and d_{yz} orbitals of the metal causing a removal of electron density from the metal. Electrons in these orbitals, which contribute negatively to the field gradient, are now delocalised into the ligand π* orbitals, and such delocalisation thereby causes an increase in the size of the field gradient at the iron nucleus.[44]

Pyridine ligands. A poor σ donor and a fair π acceptor will have a larger ΔE_Q, as for the pyridine ligands. There is good evidence that iron(II) in haemochromes acts as an electron donor and that pyridine is a π acceptor.[45] However, Cole *et al.*[46] have presented evidence suggesting that σ bonding is predominant in 4-amino- and 4-methyl-pyridine.

Imidazole ligands. The imidazole-type ligands have small ΔE_Q values in the $[Fe^{II}L^1(L')_2]$ complexes (Table 4). This is expected as in the known $[Fe^{II}(tpp)(1\text{-mim})_2]$ structure[47] the 1-methylimidazole (1-mim) ligands are close to the iron {2.014(5) Å compared with pyridine (py), 2.10(1) Å in $[Fe^{II}(tpp)(CO)(py)]$,[48] 2.037(2) Å in $[Fe^{II}(tpp)(py)_2]$[49] and 2.039(1) Å in $[Fe^{II}(tpp)(py)_2]\cdot 2py$[50]} demonstrating that the five-membered rings can get closer to the iron porphyrin plane than can the six-membered rings. Others have suggested similar steric arguments for cyclic aliphatic amines.[45b] Also, imidazole is a stronger base than pyridine and might therefore be expected to generate a smaller ΔE_Q (it will be a better σ donor than pyridine). In addition imidazole is not as good a π* acceptor as pyridine so that the delocalisation of the metal d_{xz} and d_{yz} electrons will be less; again this will tend to lower the ΔE_Q value.

Experimental justification for the simple arguments put forward to explain the bonding in $[Fe^{II}L^1(L')_2]$ complexes may be found in a recent paper by Scheidt and co-workers.[21] There,

a plot of ionisation potentials against pK_a of the conjugate acids of a series of substituted pyridines is presented. The plot shows the relative energy potentials of the lone-pair σ-symmetry orbital on the nitrogen, and the π and π* orbitals on pyridine rings. On the same plot the probable energies of the d orbitals of iron(III) are given for tpp complexes (those for oep complexes are said to be lower). The plot indicates how the energies of the π, π* and σ orbitals depend on the pK_a of the conjugate acid of the pyridine. It may be appreciated that the wide range of σ basicities leads to a systematic trend in the energies of the frontier orbitals of the axial ligands. Of course when the ligands bind the relative position of these orbitals may change. For the more basic pyridines the main π interaction may be from the filled π orbital of the pyridine into the hole in the d_π orbitals of the iron(III) (L′ to M π donation),[21] whereas for less basic pyridines the main π interaction will be from the filled $3d_\pi$ orbitals on the metal to the empty π* of the pyridine (M to L′ π back bonding). These latter arguments will only be of value if the pyridine ligands π-bond significantly with the iron; the results of this paper suggest they do not. These arguments will only differ for iron(II) porphyrins in that there is no hole in the $3d_\pi$ orbitals so only M to L′ π back bonding needs to be considered. The difference in energy of the d_π orbitals in iron(II) will in fact raise these orbitals higher so that metal back bonding will be more favourable, as seen for oep complexes.[51] It must be stated that the gas-phase ionisation[51] refers to electrons ejected from the porphyrin π system but these orbitals exhibit a remarkable metal dependence.

Amine ligands. We now compare Mössbauer spectroscopic data for the RNH_2-liganded complexes with those from the other data sets, looking for an explanation in the absence of π bonding in the former. Although the above arguments have been generated to account for the ΔE_Q values for the iron(II) compounds, similar arguments might be expected to hold good for the iron(III) compounds provided: (*a*) that the main difference between them is the electron hole in the iron(III) t_{2g} orbitals and that this has a comparable effect on ΔE_Q of all the compounds and (*b*) that the ground state is the same in all the iron(III) complexes [*i.e.* $(d_{xy})^2(d_{xz}d_{yz})^3$, $V_{zz} > 0$] considered. We can get a feel for these suppositions by comparing the differences in ΔE_Q for similar ligands between the iron-(II) and -(III) complexes, *i.e.* $D = \Delta E_Q(Fe^{III}) - \Delta E_Q(Fe^{II})$. For imidazole $D = 1.34(1)$ [solid iron(III) ΔE_Q value used], for 1-methylimidazole $D = 1.21(3)$, for *n*-octylamine $D = 0.54(3)$, for *n*-butylamine $D = 0.77(2)$ for *n*-propylamine $D = 0.40(5)$, for pyridine $D = 0.67(3)$ and for histidine $D = 0.97(6)$ mm s^{-1}. Thus the least change is seen in the aliphatic amines (except for *n*-butylamine) and for these D is around 0.5(2) mm s^{-1} and must be predominantly due to the electron hole in the t_{2g} orbitals on the iron(III). From this the effect of a simple lone pair σ-donating to the iron(III) is seen. The change for pyridine is of a very similar magnitude and may be explained in the same way. Much larger D values are found for the five-membered imidazole and histidine rings. If the imidazole ligands behave identically in the $[Fe^{III}L^1(L')_2]^+$ as in the $[Fe^{II}L^1(L')_2]$ complexes, then we would have expected ΔE_Q values equal to ΔE_Q for the corresponding iron(II) complex plus D (0.6 mm s^{-1}) giving values around 1.5 to 1.6 mm s^{-1}. The fact that all the values observed are greater than this is evidence that there is more electron donation to the metal $3d_{yz}$, $3d_{xz}$ orbital from the axial ligand π orbitals than might have been expected by comparison with the corresponding iron(II) complexes. The iron(II) $3d_{yz}$ and $3d_{xz}$ orbitals are not able to accept π-electron density from the imidazole ligands as they are filled. The imidazole ligands are thought to have stronger π-donor character than pyridine ligands.[33] Although imidazole ligands can be thought of as fairly good σ donors and poor π acceptors their properties appear to change when bound to iron(III) rather than iron(II). This change is because these ligands become good π donors to iron(III) as they can donate into the hole in the t_{2g} 3d orbital and thus enter into π bonding. This causes delocalisation of the metal t_{2g} 3d electron population and increases ΔE_Q [see equation (1)]. This change is manifest by the increase in ΔE_Q found for these iron(III) complexes. Furthermore the additional increase in ΔE_Q that is caused by changes of the axial ligand planes on going from perpendicular to parallel orientation[1,2] can now be explained, *viz.* for the case where axial ligands are perpendicular (Fig. 1), only one can enter into π bonding with the t_{2g} orbital containing the electron hole. However, when they are parallel both ligands can enter into π bonding with the orbital further delocalising the metal population and from equation (1) further increasing ΔE_Q. If this is so then supposition (*a*) holds. The question that needs to be stressed is why do only the imidazole and histidine ligands with FeL^1 behave in this way? The facts that the aliphatic amines and the simple pyridines (when not sterically hindered) and also piperidine show the least variances may well be of significance. Nature did not choose such molecules to be its haem master control. We have previously shown that hydrogen bonding to imidazoles[1,2] results in variation of ΔE_Q. If such bonding changes the π-acceptor properties of the ligand which is likely then this is a simple way of varying its electronic field at Fe^{III}. Hence the significance of histidines is demonstrated.

It is pertinent to compare the known structures of $[Fe^{III}(por)(L')_2]^+$ and $[Fe^{II}(por)(L')_2]$ compounds (L′ = an imidazole-type ligand) (Table 5). For the iron(III) structures the

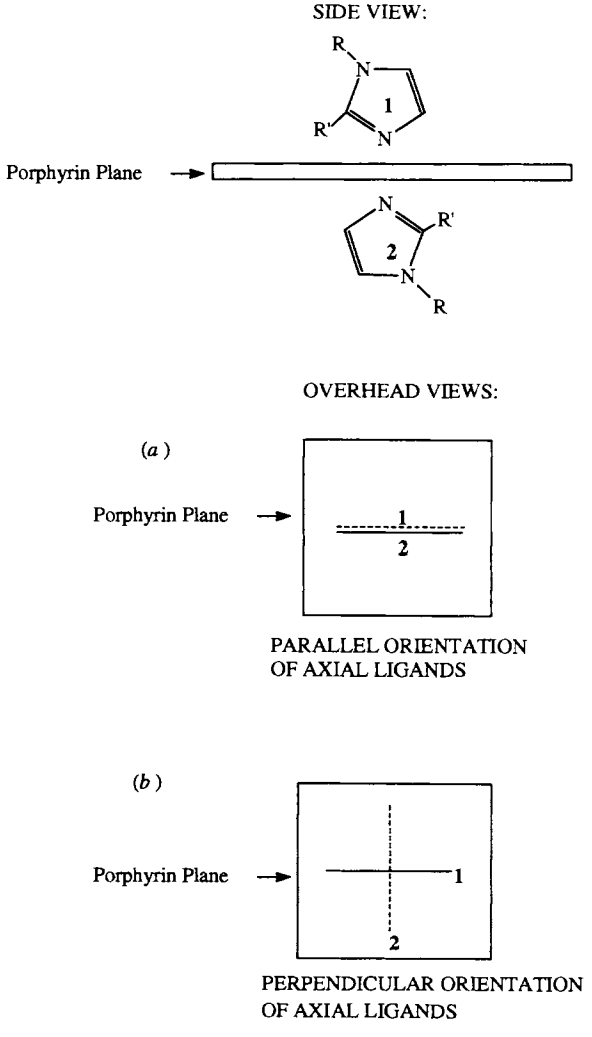

Fig. 1 Orientation of axial N-heterocycle ligands in $[Fe^{III}L^1(L')_2]$: (*a*) parallel, where L′ = imidazole, R = R′ = H; (*b*) perpendicular, where L′ = 2-methylimidazole, R = H, R′ = Me

Table 5 Summary of Fe–N bond distances for $[M(por)(L')_2]^+$ (M = Fe^{II} or Fe^{III}) structures

Complex	$Fe-N_{por}$/Å	$Fe-N_{ax}$[a]/Å	$\Delta\Phi$[b]/°	Ref.
Iron(III)				
$[Fe(tpp)(Him)_2]Cl\cdot MeOH$	1.989(8)	1.991(5)	57	52
		1.957(4)		
$[Fe(tpp)(Him)_2]Cl\cdot CHCl_3\cdot H_2O$	1.994(12)	1.977(3)	0	53
	1.993(4)	1.964(3)	0	
$[Fe(tpp)(1\text{-}mim)_2]ClO_4$	1.982(11)	1.970(3)	11	54
		1.978(3)		
$[FeL^1(1\text{-}mim)_2]ClO_4$	1.991(16)	1.988(5)	13	55
		1.966(5)		
$[Fe(tmp)(1\text{-}mim)_2]ClO_4$	1.988(20)	1.975(3)	0	21
	1.987(1)	1.965(3)	0	
$[Fe(tdcpp)(vim)_2]ClO_4$	1.978(8)	1.976(4)	6	56
		1.968(4)	76	
$[Fe(tpp)(cmu)_2]SbF_6$	1.995(17)	1.979(7)	0	57
	1.997(1)	1.967(7)		
$[Fe(tpp)(tmu)_2]SbF_6$	1.992(5)	1.983(4)	0	57
$[KL^2][Fe(tpp)(4\text{-}mim)_2]$	1.998(25)	1.928(12)	18	58
		1.958(12)		
$[Fe(tpp)(2\text{-}mim)_2]ClO_4$	1.971(4)	2.015(4)	89	60
		2.010(4)		
$[Fe(tmp)(dmapy)_2]ClO_4$	1.964(10)	1.989(4)	79	20
		1.978(4)		
$[Fe(oep)(dmapy)_2]ClO_4$	2.002(4)	1.995(3)	0	20
$[Fe(tpp)(py)_2]ClO_4$	1.982(7)	2.005(5)	86	61
		2.001(5)		
$[Fe(oep)(cpy)_2]ClO_4$	1.995(6)	2.031(2)	0	62
Iron(II)				
$[Fe(tpp)(1\text{-}mim)_2]$	1.997(6)	2.014(5)	0	47
$[Fe(tpp)(bim)_2]$	1.993(9)	2.017(4)	0	59
$[Fe(tpp)(vim)_2]$	2.001(2)	2.004(2)	0	59
$[Fe(tpp)(py)_2]\cdot 2py$	1.989(1)	2.039(1)	0	50
	1.997(1)			
$[Fe(tpp)(py)_2]$	2.001(1)	2.037(2)	0	49

Abbreviations: Him = imidazole; vim = 1-vinylimidazole; L^2 = 4,7,13,16,21,24-hexaoxa-1,10-diazabicyclo[8.8.8]hexacosane; dmapy = 4-dimethylaminopyridine; bim = 1-benzylimidazole; tdcpp = 5,10,15,20-tetrakis(2,6-dichlorophenyl)porphyrinate; cmu, tmu = *cis*-, *trans*-methyl urocanate [methyl 3-(imidazol-5-yl)prop-2-enoate]. [a] N_{ax} is from either a substituted pyridine or imidazole ligand. [b] Dihedral angle between the axial ligand planes, where each φ is the orientation angle of the closest $Fe-N_{por}$ vector and the projection of the axial ligand plane on the porphyrin plane.

axial bond lengths to the non-sterically hindered imidazole-type ligand are in the range 1.928(12)–1.991(5) Å with an average of 1.970(5) Å (for nine structures)[21,52–58] whereas those for the iron(II) structures are 2.004(2)–2.014(5) Å with an average of 2.009(5) Å (for three structures).[47,59] Thus the overall average change in the imidazole axial Fe–N bond between Fe^{II} and Fe^{III} is *ca.* 0.04 Å. It therefore appears that there is a shortening of this bond for the iron(III) structures. Where it is least changed in the case of the 2-mim compounds (where the axial ligands suffer steric hindrance)[47,60] then D is 0.61(6) mm s^{-1} comparable to values for the aliphatic amines and implying no π interactions.

For the pyridine structures the axial Fe^{II}–N bond length range is 2.037(2)–2.039(1) Å,[49,50] this is 0.032(2) Å larger than that for the corresponding iron(III) compound.[61] We note that for $[Fe^{III}(oep)(cpy)_2]ClO_4$ (cpy = 3-chloropyridine) the axial Fe–N bond length is 2.031(2) Å.[62]

The average axial Fe–N difference distances for the iron-(II) and -(III) structures with imidazole and pyridine ligands are thus the same within experimental error. Taken together these facts suggest that the axial ligand bond lengths do not provide direct evidence for bonding changes. Hence no obvious structural differences can be linked to the differences in D.

It is thus apparent that the Mössbauer spectroscopic data for the low-spin iron-(II) and -(III) complexes of the aliphatic amine allow the establishment of a base value for axial ligand σ-bonding effects. The highest ΔE_Q value for the $Fe^{III}L^1$ complexes of non-cyclic aliphatic amines is 1.80(3) mm s^{-1}. This is only a little less than those of the sterically hindered imidazole ring complexes where the rings are perpendicular to each other [1.87(2) mm s^{-1} for 2-mim, Table 3].

A recent paper by Walker and co-workers[63] discussed $[Fe^{III}(tpp)(cnpy)_2]ClO_4$ (cnpy = 4-cyanopyridine) (ΔE_Q = 0.65 mm s^{-1}) and found that the ground-state configuration is $(d_{xz}, d_{yz})^4(d_{xy})^1$ which is quite different from those for the compounds used in this work and those we have discussed above. We have previously suggested that in $Na[Fe^{III}L^1(CN)_2]$ (ΔE_Q = 0.53 mm s^{-1}) the ground state is $(d_{xz}, d_{yz})^4(d_{xy})^1$.[64] We note that in the limit for a 'pure' $(d_{xz}, d_{yz})^4(d_{xy})^1$ ground state, where there is no contribution to the wavefunction of the unpaired electron due to spin–orbit coupling, we would expect $g_{xx} = g_{yy} = g_{zz} = 2$.[63] Thus an EPR signal similar to those of organic free radicals would be observed in the limit $\Sigma g^2 = 12$.[63] As will be seen in the following section and Table 6 our smallest $\Sigma g^2 = 14.75$ and the largest is equal to 15.63 which is close to the maximum, expected $\Sigma g^2 = 16$ for a 'pure' $(d_{xy})^2(d_{xz},d_{yz})^3$ ground state.[65]

EPR results for low-spin iron(III) complexes

The species of interest, monomeric low-spin complexes, give strong EPR spectra with $g_x \approx 1.9, g_y \approx 2.2$ and $g_z \approx 2.5$ (Table 6) (for a typical spectrum see Fig. 2). All systems studied gave similar features except the ethylamine system, but in some cases the features were too broad to measure accurate g values, even using computer simulation.

The g values. For low-spin iron(III) complexes, EPR spectroscopy gives the three g values directly. Generally for near-octahedral ligand binding the electrons are confined to the π* orbitals which are largely centred on d_{xy}, d_{xz} and d_{yz} orbitals on the metal. For haem derivatives, the d_{xy} orbital is usually treated as being almost non-bonding, and is therefore the lowest

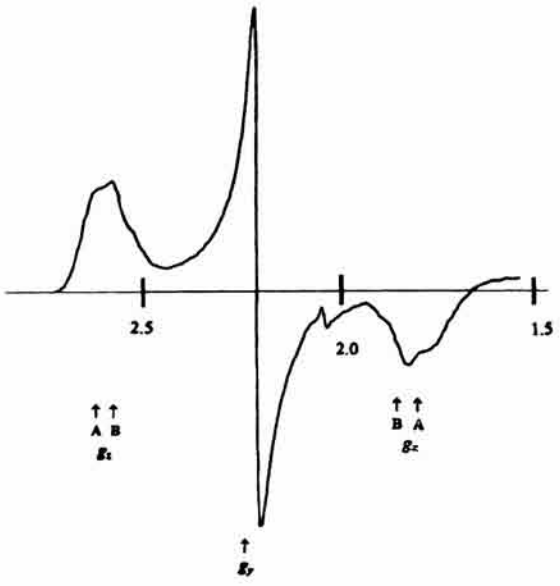

Fig. 2 First-derivative X-band EPR spectrum for $[Fe^{III}L^1(pip)_2]^+$ (pip = piperidine) recorded at 77 K, showing features for complexes A and B. Microwave frequency 9219 GHz, power 10 mW, modulation amplitude 5 G (5×10^{-4} T)

Table 6 The EPR data for $[Fe^{III}L^1(L')_2]^+$ (A and B centres) prepared in this work, recorded at X-band at 77 K

	Centre A			Centre B		
L'	g_z	g_y	g_x	g_z	g_y	g_x
Ethylamine	2.7[a]	2.2	*ca.* 1.9			
Diethylamine[b]						
Triethylamine[b]						
1,2-Diaminoethane		2.23[a]				
n-Propylamine[c]				2.51	2.2	1.90
n-Butylamine[d]				2.54	2.2	1.87
n-Octylamine	2.72	2.22	1.82			
n-Decylamine	2.70	2.2	1.80	2.57	2.2	1.87
n-Dodecylamine	2.73	2.2	1.83	2.60	2.2	1.90
Piperidine	2.64	2.22	1.79	2.55	2.22	1.85
Morpholine	2.68[a]	2.2	1.83	2.54	2.2	1.87
Mean	2.7	2.2	1.81	2.55	2.2	1.88

[a] Broad. [b] Only high-spin features detected. [c] Weak. Centre g values of 2.15, 2.10 and 2.00. [d] Also weak second centre had g values of 2.30, 2.15 and 1.95.

of the three. In axial symmetry the d_{xz},d_{yz} pair are degenerate, but will be split by distortions of various sorts, and by π bonding. Nevertheless spin–orbit coupling between the orbitals is often quite strong, and is usually the major factor contributing to the g shifts. This leads to the configuration d_{xy}^2, d_{yz}^2, d_{xz}^1. If the d_{xy} orbital and σ-orbitals are well removed from the xz–yz pair, then for the magnetic field along z, the xz–yz orbitals couple and there is a large shift to high g values, moving towards the limit of g_z ($g_\parallel$) = 4. Fields along x and y do not couple these levels, but in the absence of other significant coupling there is a shift for g_x and g_y towards the limiting value of $g_x = g_y = g_\perp = 0$. This is a direct consequence of the orbital motion around z, and begins to become important when $g_z \geqslant 2.5$.

However, if the d_{xy} orbital is not too far removed, for the field along y, the yz and xy orbitals couple and because the xy orbital is filled this induces a positive shift for g_y. Hence the usual pattern of g values is $g_z \gg 2.0$, $g_y \approx 2.0$ and $g_x < 2.0$. This is displayed in Fig. 3 for a series of haem complexes in Table 7.[17,20,53,54,56,57,58,66] Here the values for g_z are arbitrarily placed on a 45° line, purely for display purposes. The sharp

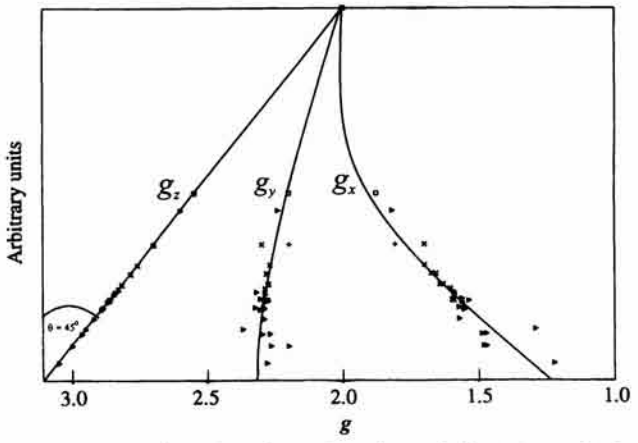

Fig. 3 Range of g values for various low-spin iron(III) porphyrin complexes based on literature data for solid-state imidazole (▷) and pyridine derivatives (×) given in Table 7 and showing our results for saturated aliphatic amines [centres A(+) and B(□)]. The g_z values were placed on the 45° line for display purposes only: the vertical axis has no specific significance

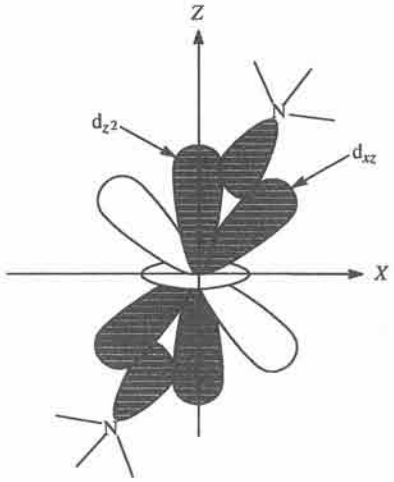

Fig. 4 Sideways bonding of aliphatic amine ligands to the d_{xz}/d_{yz} orbitals as well as to the d_{z^2} orbital. The aliphatic ligand has been moved far off the z axis as an exaggeration to clarify the envisaged bonding

trend to low g values is clearly seen for g_x, but g_y values all come quite close to 2.2 for the selected data.

Structurally, the most informative g value is therefore g_z. For the planar ring ligands one controlling factor seems to be the relative orientation of the rings, those with rings perpendicular giving very large shifts (≈3.3–3.5) and those with rings parallel giving smaller shifts (≈2.5–3.0) (Fig. 1). In many cases the orientations lie between these limits, and so do the g_z values. It seems that for θ ≈ 90°, d_{xz} and d_{yz} are equally involved in π bonding and hence the splitting is small. For θ ≈ 0° there is a preference for only one of the d orbitals for π bonding, and hence the splitting is large.

In the light of these arguments our results for the amines are remarkable, with g_z values in the lowest region (≈2.5). Normal π–π bonding is now impossible, and σ–π delocalisation, which is expected to be weak, should not show any large discrimination between N–C and N–H bonds. We had therefore expected near orbital degeneracy with g_z values ≈3.5 or higher. No such features were observed.

We tentatively suggest that the axial ligands have shifted sideways such that there is significant σ overlap with the d_{xz} or d_{yz} orbitals and reduced overlap with the d_{z^2} orbital (Fig. 4). These shifts (or tilts) can be *cis* or *trans* but a *trans* distortion seems to us to be more probable. This will push the antibonding d_{xz} orbital above the d_{yz} orbital thereby quenching orbital angular momentum and shifting g_z towards 2.00. The source of

this distortion is probably the bulky R group in the RNH_2 ligands. It may be significant that with ethylamine the EPR features were either too broad to detect or, for some reason, the complex failed to form. Since the g values are so strongly dependent on the extent of distortion it may be that in this case the distortion is less precise, giving a spread of g values and hence broad lines. The suggestion of the axial ligands shifting sideways causing σ overlap with the d_{xz} and/or d_{yz} orbitals may help to explain the high value of ΔE_Q observed for the *n*-butylamine complex if in this complex such overlap is maximised, and leads to (parallel) interactions involving only one of the t_{2g} orbitals.

The fact that in many cases two low-spin complexes were detected (A and B) with similar g values suggests that there is arbitrariness in the selection of specific directions for these distortions. On the other hand, the fact that *only* one or two species were detected suggests that the distortions are well defined. In the particular case of the ethylamine derivative for which no resolved g features were observed, we suggest that no such well defined pathways were required to accommodate the steric effects of the ethyl groups.

In all these experiments the solvents were mixtures of amines with methanol or ethanol, selected because they give good glasses on freezing, with no phase separation. In another series of experiments the amine alone was the solvent. Under such conditions, when the amine was the solvent, mixed axial ligands such as one solvent molecule plus one amine molecule are ruled out; also, the EPR spectra were similar for different solvent systems.

Some spectra showed, in addition to the A and B features, weak features in the range g 2.35–1.95. These results establish that compounds 'A' and 'B' were not mixed species with one amine and one solvent ligand rather than two amine ligands. It should be noted that species A and B are very similar, causing slightly different splitting of the d_{xz}–d_{yz} pair and slightly different EPR spectra. The Mössbauer ΔE_Q values are only sensitive to differences in electron populations not to the magnitude of the splittings and would not be expected to differentiate between two such similar species.

Other active centres. In a few cases, $g = 6$ features were present for axial high-spin iron(III) species. This was also the case in the work on N-aromatic ligands[16] and is attributed to impurities rather than a switch in spin state. We also often detected signals which we attribute to μ-oxo dimers: this will be described and discussed elsewhere.

Conclusion

Mössbauer, EPR and electronic spectral data have been presented that confirm the formation of new low-spin $[Fe^{III}L^1(L')_2]$ complexes (L′ = an aliphatic primary amine or secondary cyclic amine).

The Mössbauer data for these compounds when compared with those for their iron(II) analogues as well as those for the pyridine, imidazole and histidine complexes (both Fe^{II} and Fe^{III}) facilitate a better understanding of the nature of the bonding in these compounds. It was demonstrated that the $[Fe^{III}L^1(L')_2]$ complexes (L′ = aliphatic amines) generate ΔE_Q values of similar magnitude. The imidazole ligands had very much larger ΔE_Q values than might have been expected by reference to the iron(II) complexes. The larger ΔE_Q values found for the $[Fe^{III}L^1(L')_2]$ (L′ = imidazole) complexes for the case where the ligand planes are nearly parallel arises from enhanced π-electron donation to the hole in the t_{2g} 3d orbital from both the imidazole ligands. For the case where the imidazole ligands are closer to perpendicular only one iron 3d orbital (the one with the single electron) will be able to π bond as the other being filled cannot accept π-electron density from the imidazole ligand.

From comparisons between the Mössbauer data of $[Fe^{II}L^1(L')_2]$ and $[Fe^{III}L^1(L')_2]$ complexes the following points are apparent. (1) For iron(III) complexes where L′ = primary aliphatic amine the ΔE_Q values are of similar magnitude. (2) The increase in ΔE_Q in going from iron(II) to iron(III) is of the same order for primary aliphatic amines, cyclic secondary amines (piperidine) and pyridine suggesting the main controlling factor is the loss of one electron in the $(d_{xz}, d_{yz})^3$ orbitals. (3) The corresponding change in ΔE_Q for histidine and imidazole to that of point (2) is significantly larger, but without the current work there would have been no way to appreciate this. The increase suggests that the mode of bonding of these ligands changes and back bonding becomes important for the iron(III) complexes. It is this back bonding that if modulated may facilitate control of the iron chemistry. It has been postulated that such modulation could be achieved through manipulation of the hydrogen bonding to the imidazole or histidine.[1,2] Such manipulation could obviously not be carried

Table 7 The EPR data for $[Fe^{III}(por)(L')_2]^+$ complexes where L′ = pyridine or imidazole derivative (frozen-solution data, solvent CH_2Cl_2) unless otherwise stated

Complex[a]	T/K	g_1	g_2	g_3	Ref.
Pyridine derivatives					
[Fe(tpp)(dmampy)$_2$]I	77	2.865	2.286	1.591	17
[Fe(tpp)(dapy)$_2$]I	77	2.864	2.280	1.597	17
[Fe(tpp)(apy)$_2$]I	77	2.830	2.289	1.603	17
[Fe(oep)(dmapy)$_2$]ClO_4	25	2.818	2.278	1.642	20
(crystalline data)	25	2.818	2.275	1.630	20
[Fe(tpp)(dmapy)$_2$]I	77	2.786	2.284	1.657	17
[Fe(tpp)(dmadmpy)$_2$]I	77	2.785	2.281	1.675	17
[Fe(tdcpp)(apy)$_2$]ClO_4	77	2.76	2.27	1.70	20
[Fe(tdcpp)(dmapy)$_2$]ClO_4	77	2.70	2.30	1.70	20
(crystalline data)					
Imidazole derivatives					
[Fe(ttepp)(Him)$_2$]Cl	4.2	3.05	2.28	1.22	66
[Fe(tpp)(Him)$_2$]Cl·$CHCl_3H_2O$[b]	6	3.00	2.2	1.47	53
(crystalline data)					
[Fe(tpp)(cmu)$_2$]SbF_6[b]	77	2.999	2.265	1.481	57
(single-crystal data)	77	2.965	2.298	1.486	57
[Fe(tpp)(tmu)$_2$]SbF_6	77	2.964	2.269	1.471	57
(single-crystal data)					
[Fe(ttipp)(Him)$_2$]Cl	4.2	2.95	2.37	1.29	66
[Fe(ttmpp)(Him)$_2$]Cl	4.2	2.92	2.29	1.57	66
[Fe(tdcpp)(vim)$_2$]ClO_4	7	2.90	2.27	1.57	56
(single-crystal data)					
[Fe(tpp)(pim)$_2$]I	77	2.893	2.307	1.552	17
[Fe(tpp)(1-mim)$_2$]ClO_4	77	2.890	2.291	1.554	54
(crystalline data)					
[Fe(tmp)(1-mim)$_2$]ClO_4	25	2.886	2.325	1.571	20
[Fe(tpp)(1-mim)$_2$]I	77	2.886	2.294	1.549	17
[Fe(tdcpp)(vim)$_2$]ClO_4	7	2.88	2.27	1.57	56
(microcrystalline data)					
(frozen-solution data)	7	2.88	2.30	1.57	56
[Fe(tpp)(Him)$_2$]Cl	4.2	2.87	2.29	1.56	17
[Fe(tpp)(1-mim)$_2$]ClO_4	77	2.866	2.276	1.535	54
(crystalline data)					
[Fe(tpp)(bim)$_2$]I	77	2.860	2.306	1.561	17
[Fe(tpp)(4-mim)$_2$]I	77	2.847	2.288	1.590	17
[Fe(tpp)(Him)$_2$]Cl·$CHCl_3H_2O$[b]	6	2.84	2.32	1.59	53
(crystalline data)					
[KL^2][Fe(tpp)(4-mim)$_2$]	77	2.60	2.24	1.82	58
(frozen solution in dimethylacetamide)					
(crystalline data)	77	2.60	2.24	1.82	58

[a] dmampy = 4-dimethylamino-3-methylpyridine; dapy = 3,4-diaminopyridine; apy = 4-aminopyridine; dmadmpy = 4-dimethylamino-3,5-dimethylpyridine; pim = 4-phenylimidazole; ttepp = 5,10,15,20-tetrakis(2,4,6-triethylphenyl)porphyrinate; ttipp = 5,10,15,20-tetrakis(2,4,6-triisopropylphenyl)porphyrinate; ttmpp = 5,10,15,20-tetrakis(2,4,6-trimethylphenyl)porphyrinate. [b] Two overlapping EPR signals obtained in the solid state.

out on aliphatic amines (which do not have π and π^* orbitals) or single nitrogen rings such as pyridine.

The EPR spectra for the new low-spin $[Fe^{III}L^1(L')_2]$ (L' = aliphatic amine) complexes give evidence for a sideways shift of the axial ligands such that there is significant σ overlap with d_{xz} or d_{yz} orbitals and reduced overlap with the d_{z^2} orbital. This shift led to g_z values ≈ 2.5 similar to those found for the parallel ligand orientation for N-heterocyclic ligands. It is suggested that these shifts are steric requirements of the ligands rather than a bonding preference. The fact that some evidence for σ bonding of the ligands with metal d_{xz} and/or d_{yz} orbitals has been found indicates that previous ideas of bonding in $[Fe^{III}(por)(L')_2]^+$ species, where electron-pair donation to the $3d_{z^2}$ orbital alone was considered, may have been oversimplified.

Acknowledgements

We thank Dr. J. R. Miller of this department for useful discussions, and the referees for their comments. As pointed out by the referees, the ammonia complex would be a good test of the ideas addressed in this work, but as discussed we have not been able to synthesise it.

References

1 O. K. Medhi and J. Silver, *J. Chem. Soc., Dalton Trans.*, 1990, 263.
2 O. K. Medhi and J. Silver, *J. Chem. Soc., Dalton Trans.*, 1990, 555.
3 G. R. Moore and R. J. P. Williams, *FEBS Lett.*, 1977, **79**, 229.
4 F. S. Matthews, E. W. Czerwinski and P. Argos, in *The Porphyrins*, ed. D. Dolphin, Academic Press, New York, 1979, vol. 7, pp. 108–147.
5 T. Iyangi, *Biochemistry*, 1977, **16**, 2725.
6 W. R. Widger, W. A. Cramer, R. G. Herriman and A. Trebst, *Proc. Natl. Acad. Sci. USA*, 1984, **81**, 674.
7 G. T. Babcock, W. R. Widger, W. A. Cramer, W. A. Oertlings and J. Mertz, *Biochemistry*, 1985, **24**, 3638.
8 R. Keller, O. Groudinsky and K. Wüthrich, *Biochim. Biophys. Acta*, 1973, **328**, 233.
9 W. E. Blumberg and J. Peisach, in *Cytochrome Oxidase*, eds. T. E. King, Y. Orii, B. Chance and K. Okuniki, Elsevier, Amsterdam, 1979, pp. 153–159.
10 G. T. Babcock, P. M. Callahan, M. R. Ondrias and I. Salmeen, *Biochemistry*, 1981, **20**, 959.
11 M. F. Perutz and L. F. Ten Eytuck, *Cold Spring Harbor Symp. Quant. Biol.*, 1971, **36**, 295.
12 J. C. Salerno, *J. Biol. Chem.*, 1984, **259**, 2331.
13 A.-L. Tsai and G. Palmer, *Biochim. Biophys. Acta*, 1983, **722**, 349.
14 K. R. Carter, A. Tsai and G. Palmer, *FEBS Lett.*, 1981, **132**, 243.
15 D. L. Brautigan, B. A. Feinberg, B. M. Hoffman, E. Margoliash, J. Peisach and W. E. Blumberg, *J. Biol. Chem.*, 1977, **252**, 574.
16 F. A. Walker, B. H. Hunyh, W. R. Scheidt and S. R. Osvath, *J. Am. Chem. Soc.*, 1986, **108**, 5288.
17 F. A. Walker, D. Reis and V. L. Balke, *J. Am. Chem. Soc.*, 1984, **106**, 6888.
18 W. R. Scheidt and D. M. Chipman, *J. Am. Chem. Soc.*, 1986, **108**, 1163.
19 M. F. Slifkin, in *Charge Transfer Interaction of Biomolecules*, Academic Press, London, 1971, ch. 6.
20 M. K. Safo, G. P. Gupta, F. A. Walker and W. R. Scheidt, *J. Am. Chem. Soc.*, 1991, **113**, 5497.
21 M. K. Safo, G. P. Gupta, C. T. Wilson, U. Simonis, F. A. Walker and W. R. Scheidt, *J. Am. Chem. Soc.*, 1992, **114**, 7066.
22 T. A. Kent, E. Münck, W. R. Dunham, W. F. Filter, K. L. Findling, T. Yoshida and J. A. Fee, *J. Biol. Chem.*, 1982, **275**, 12 489.
23 J. Peterson, J. Silver, M. T. Wilson and I. E. G. Morrison, *J. Inorg. Biochem.*, 1980, **13**, 75.
24 J. Peterson, M. M. M. Saleem, J. Silver, M. T. Wilson and I. E. G. Morrison, *J. Inorg. Biochem.*, 1983, **19**, 165.
25 P. Adams, R. C. de L. Milton and J. Silver, *Biometals*, 1994, **7**, 217.
26 T. A. Kent, L. J. Young, G. Palmer, J. A. Fee and E. Münck, *J. Biol. Chem.*, 1983, **258**, 8543.
27 E. Munck, *Methods Enzymol.*, 1978, **54**, 14 341.
28 O. K. Medhi and J. Silver, *Inorg. Chim. Acta*, 1989, **164**, 231.
29 M. T. Ahmet, G. Al-Jaff, J. Silver and M. T. Wilson, *Inorg. Chim. Acta*, 1991, **183**, 43.
30 G. Al-Jaff, J. Silver and M. T. Wilson, *Inorg. Chim. Acta*, 1990, **176**, 307.
31 (*a*) H. Davies, *J. Biol. Chem.*, 1940, **135**, 643; (*b*) H. M. Marques, O. Q. Munro and M. L. Crawcour, *Inorg. Chim. Acta*, 1992, **96**, 221; (*c*) H. M. Marques, M. P. Byfield and J. M. Pratt, *J. Chem. Soc., Dalton Trans.*, 1993, 1633; (*d*) M. P. Byfield, M. P. Hamza and J. M. Pratt, *J. Chem. Soc., Dalton Trans.*, 1993, 1641; (*e*) M. S. A. Hamza and J. M. Pratt, *J. Chem. Soc., Dalton Trans.*, 1994, 1367; (*f*) M. S. A. Hamza and J. M. Pratt, *J. Chem. Soc., Dalton Trans.*, 1994, 1377.
32 (*a*) J. Silver and B. Lukas, *Inorg. Chim. Acta*, 1983, **78**, 219; (*b*) M. Y. Hamed, R. C. Hider and J. Silver, *Inorg. Chim. Acta*, 1982, **66**, 13.
33 (*a*) C. E. Castro, M. Jamin, W. Yokoyama and R. Wade, *J. Am. Chem Soc.*, 1986, **108**, 4179; (*b*) L. M. Epstein, D. K. Straub and C. Marricondi, *Inorg. Chem.*, 1967, **6**, 1720.
34 F. M. Jones III and E. A. Arnett, *Prog. Phys. Org. Chem.*, 1974, **11**, 26; D. A. Aue, H. M. Webb and M. T. Bowers, *J. Am. Chem. Soc.*, 1976, **98**, 318.
35 O. K. Medhi and J. Silver, *Inorg. Chim. Acta*, (*a*) 1989, **166**, 129; (*b*) 1990, **168**, 271.
36 M. Zerner, M. Gouterman and H. Kobayashi, *Theor. Chim. Acta*, 1966, **6**, 363.
37 J. P. Collman, J. L. Hoard, N. Kim, G. Lang and C. A. Reed, *J. Am. Chem. Soc.*, 1975, **97**, 2616.
38 J. R. Sams and T. B. Tsin, *Chem. Phys. Lett.*, 1975, **25**, 299.
39 T. B. Tsin, Ph.D. Thesis, University of British Columbia, 1975.
40 D. Dolphin, J. R. Sams, T. B. Tsin and K. L. Wong, *J. Am. Chem. Soc.*, 1976, **98**, 6970.
41 (*a*) H. Eicher and A. Trautwein, *J. Chem. Phys.*, 1969, **50**, 2540; (*b*) B. H. Huynh, D. A. Case and M. Karplus, *J. Am. Chem. Soc.*, 1977, **99**, 6013; (*c*) D. A. Case, B. H. Huynh and M. Karplus, *J. Am. Chem. Soc.*, 1979, **101**, 4433; (*d*) S. F. Sontum, D. A. Case and M. Karplus, *J. Chem. Phys.*, 1983, **79**, 2881.
42 D. Rhynard, G. Lang and K. Spartalian, *J. Chem. Phys.*, 1979, **71**, 3715.
43 G. M. Bancroft and R. H. Platt, *Adv. Inorg. Chem. Radiochem.*, 1972, **15**, 59.
44 B. W. Dale, R. J. P. Williams, P. R. Edwards and C. E. Johnson, *Trans. Faraday Soc.*, 1968, **64**, 620.
45 (*a*) W. M. Connor and D. K. Straub, *Ann. N. Y. Acad. Sci.*, 1973, **206**, 390; (*b*) D. K. Straub and W. M. Connor, *Ann. N. Y. Acad. Sci.*, 1973, **200**, 383.
46 S. J. Cole, G. C. Curthoys and E. A. Magnusson, *J. Am. Chem. Soc.*, 1970, **92**, 2991; 1971, **93**, 2153.
47 W. L. Steffen, H. K. Chun, J. L. Hoard and C. A. Reed, 175th National Meeting of the American Chemical Society, Anachem, CA, March 1978, Abstr. INOR 15.
48 S. M. Peng and J. A. Ibers, *J. Am. Chem. Soc.*, 1976, **98**, 8032.
49 N. Li, P. Coppens and J. Landrum, *Inorg. Chem.*, 1988, **27**, 482.
50 N. Li, V. Petrieck, P. Coppens and J. Landrum, *Acta Crystallogr., Sect. C*, 1985, **41**, 902.
51 S. Kitagawa, I. Morishima, T. Yonezawa and N. Sato, *Inorg. Chem.*, 1979, **18**, 1345.
52 D. M. Collins, R. Countryman and J. L. Hoard, *J. Am. Chem. Soc.*, 1972, **94**, 2066.
53 W. R. Scheidt, S. R. Osvath and Y. J. Lee, *J. Am. Chem. Soc.*, 1987, **109**, 1958.
54 T. Higgins, M. K. Safo and W. R. Scheidt, *Inorg. Chim. Acta*, 1991, **178**, 261.
55 R. G. Little, K. R. Dymock and J. A. Ibers, *J. Am. Chem. Soc.*, 1975, **97**, 4532.
56 K. Hatano, M. K. Safano, F. A. Walker and W. R. Scheidt, *Inorg. Chem.*, 1991, **30**, 1643.
57 R. Quinn, J. S. Valentine, M. P. Byrn and C. E. Strouse, *J. Am. Chem. Soc.*, 1987, **109**, 3301.
58 R. Quinn, C. E. Strouse and J. S. Valentine, *Inorg. Chem.*, 1983, **22**, 3934.
59 M. K. Safo, W. R. Scheidt and G. P. Gupta, *Inorg. Chem.*, 1990, **29**, 626.
60 W. R. Scheidt, J. L. Kirner, J. L. Hoard and C. A. Reed, *J. Am. Chem. Soc.*, 1987, **109**, 1963.
61 D. Innis, S. M. Soltis and C. E. Strouse, *J. Am. Chem. Soc.*, 1988, **110**, 5644.
62 W. R. Scheidt, D. K. Geiger and K. J. Haller, *J. Am. Chem. Soc.*, 1982, **104**, 495.
63 M. K. Safo, F. A. Walker, A. M. Raitsimring, W. P. Walters, D. P. Dolata, P. G. Debrunner and W. R. Scheidt, *J. Am. Chem. Soc.*, 1994, **116**, 7760.
64 B. Lukas and J. Silver, *Inorg. Chim. Acta*, 1986, **124**, 97.
65 J. S. Griffith, *Proc. R. Soc. London, Ser. A*, 1956, **253**, 23.
66 M. Nakamura, K. Tajima, K. Tada, K. Ishizu and N. Nakamura, *Inorg. Chim. Acta*, 1994, **224**, 113.

Received 11*th December* 1995; *Paper* 5/08055J